ENGLISH VERSION

Calibration of an empirical model for moisture content assessment and monitoring in compacted tropical soils used in the subgrade of road pavements

Calibración de un modelo empírico para la evaluación y monitoreo del contenido de humedad en suelos tropicales compactados usados en la subrasante de pavimentos

I. Pizarro [1]*, M. Françoso **, L. De Almeida **, E. Matsura **

* Instituto Tecnológico de Costa Rica – Cartago, COSTA RICA
** Universidade Estadual de Campinas (UNICAMP) – Campinas, BRASIL

Fecha de Recepción: 28/08/2020
Fecha de Aceptación: 15/11/2020
PAG 275-286

Abstract

Subgrade moisture variation monitoring and control is important due to its influence on road pavement performance and service life. The precise application of non-invasive techniques such as time domain reflectometry (TDR) and ground penetration radar (GPR) in compacted tropical soils depend on calibration models, that consider their mineralogical composition and geotechnical properties. The present work aims to determine calibration models that relate dielectric permittivity with moisture variation in compacted tropical soils. TDR technique was used with low-cost probes and soil calibration columns developed at laboratory for reading dielectric permittivity and define its relationship with moisture. Results showed that through laboratory standardized procedures, it is possible to determine calibration models according to the required accuracy in moisture control in the subgrade. It was found that the high density and magnetic properties of tropical soils significantly influenced the determination of dielectric permittivity and consequently in moisture estimates, hence reaffirming the need of specific calibrations for these types of soils.

Keywords: *Tropical soils; moisture content; dielectric permittivity; calibration model, TDR*

Resumen

El monitoreo y control de la variación de humedad de la subrasante es importante debido a su influencia en el desempeño y vida de servicio del pavimento. La aplicación precisa de técnicas no invasivas como la reflectometria en el dominio del tiempo (TDR) y el radar de penetración terrestre (GPR) en suelos tropicales compactados, dependen de modelos de calibración que consideren su composición mineralógica y propiedades geotécnicas. El presente trabajo tiene como objetivo determinar modelos de calibración que relacionen la permitividad dieléctrica con la variación de humedad en suelos tropicales compactados. La técnica TDR se utilizó con sondas de bajo costo y columnas de calibración desarrolladas en laboratorio para la lectura de la permitividad dieléctrica y definir su relación con la humedad. Los resultados demostraron que, a través de procedimientos estandarizados de laboratorio, es posible determinar modelos de calibración acordes con la precisión requerida en el control de la humedad en la subrasante. Se constató que la alta densidad y las propiedades magnéticas de los suelos tropicales, influenciaron significativamente en la determinación de la permitividad dieléctrica y, en consecuencia, en la estimación de humedad, lo que reafirma la necesidad de calibraciones específicas para este tipo de suelos.

Palabras clave: Suelos tropicales; contenido de humedad; permitividad dieléctrica; modelo de calibración, TDR

1. Introduction

Moisture is considered an important variable in road pavement and subgrade performance. Pavement rapid deterioration under traffic conditions is directly related to variations and excessive moisture accumulation in the subgrade and in pavement constituent layers (Bastos, 2013).

Time Domain Reflectometry (TDR) and Ground Penetrating Radar (GPR) are non-destructive methods commonly used for real time measurement and monitoring the soil moisture content and consequently in pavement and subgrade. These electromagnetic methods are useful when samples and the site under observation need to be preserved and generally employed in monitoring situations over time, aiming to assess and visualize moisture seasonal variations. Examples of studies employing both techniques to estimate and monitor moisture in civil engineering materials and structures are shown below: (Klemunes, 1998), (Jiang and Tayabji, 1999), (Al-Qadi et al., 2004), (Ekblad and Isacsson, 2007), (Benedetto, 2010), (Khakiev et al., 2014), (Thring et al., 2014), (Benedetto et al., 2015), (Tosti and Slob, 2015), (Fernandes et al., 2017) and (Bhuyan et al., 2018).

[1] ***Corresponding author:***
Instituto Tecnológico de Costa Rica – Cartago, COSTA RICA
E-mail: ipizarro@itcr.ac.cr

TDR and GPR methods depend on the same electromagnetic properties: dielectric permittivity (ε), electrical conductivity (σ) and magnetic permeability (μ). Both are based on similar electromagnetic wave propagation principles (Curioni et al., 2017) to determine dielectric permittivity in a first stage and later moisture content, by using calibration models. The precision in moisture content estimates in the subgrade require specific calibration models for compacted tropical soils, which take into consideration their mineralogical composition, in addition to their geotechnical properties. The use of existing models developed for other purposes and applications can lead to an inaccurate estimate of moisture content.

The relationship between dielectric permittivity and moisture content, for most mineral soils, does not vary substantially among different soil textures (under natural density conditions) (Roth et al., 1992). However, (Robinson et al.,1994) reported that soils with magnetic minerals can show different dielectric properties in comparison with non-magnetic mineral soils. It is common in the Brazilian territory that tropical soils present magnetic properties (magnetic susceptibility ($x_m > 0$)), which can influence dielectric permittivity measurement using electromagnetic methods and consequently affect the precision in the moisture content estimation (Souza et al., 2001).

This study aims to determine calibration models which allow relating dielectric permittivity (ε_r) with moisture content (θ_v) variation in compacted tropical soils. Six different types of soil were collected from the subgrade of road works and subjected to tests for their physical, chemical and dielectric characterization. TDR technique was used with low-cost probes and soil calibration columns, developed at Unicamp Non-Destructive Research Laboratory (LIND) for dielectric permittivity reading and acquisition.

2. Theoretical Framework

2.1 Soil electrical properties and water influence

Soil is a heterogeneous medium consisting of three phases (air, solid and liquid). The difference in the dielectric permittivity between the phases (ε_{air}= 1, $\varepsilon_{particle}$= 3-5 and ε_{water}= 81) is the main reason for the success in soil moisture content estimates using electromagnetic techniques (Huisman et al., 2003). This great contrast between the dielectric permittivity values ($\varepsilon_{particle} < \varepsilon_{water}$) is due to the high capacity of water molecules to polarize, when compared to the capacity of soil particles (Thring et al., 2014). Therefore, water is considered the most influential component in determining dielectric permittivity in soil (Saarenketo, 2006).

2.2 Calibration models that relate dielectric permittivity (ε_r) and moisture content (θ_v)

(Ekblad and Isacsson, 2007) affirm that equations or models can be theoretical, empirical and theoretical-empirical. The widely used empirical model, and probably mostly quoted, was developed by (Topp et al., 1980), as shown in the expression below, (Equation 1).

$$\theta_v = -5{,}3\text{x}10^{-2} + 2{,}92\text{x}10^{-2}\varepsilon_r - 5{,}5\text{x}10^{-4}\varepsilon_r^2 + 4{,}3\text{x}10^{-6}\varepsilon_r^3 \qquad (1)$$

Where:
θ_v = volumetric moisture content [cm^3cm^{-3}];
ε_r = relative dielectric permittivity.

(Ledieu et al., 1986) used a different approach to develop their calibration model. The authors related the electromagnetic wave travelling time with moisture content variation in compacted soil samples with a bulk density between 1,38 and 1,78 g cm^{-3}. The model is shown in the following expression (Equation 2).

$$\theta_v = 5{,}688t - 3{,}38\rho_b - 15{,}29 \qquad (2)$$

Where:
θ_v = volumetric moisture content [%];
t = electromagnetic wave travelling time [ns];
ρ_b = bulk density [g/cm^3].

2.3 Time domain reflectometry (TDR)

The technique uses electromagnetic (EM) pulses sent through a coaxial cable to a probe, normally with two or three metal rods (Figure 1). Part of the pulse is reflected due to the impedance difference of the probe in contact with the soil. Displacement time and reflection coefficient of the pulse are established, to later estimate the relative dielectric permittivity (ε_r) and the soil electrical conductivity (σ).

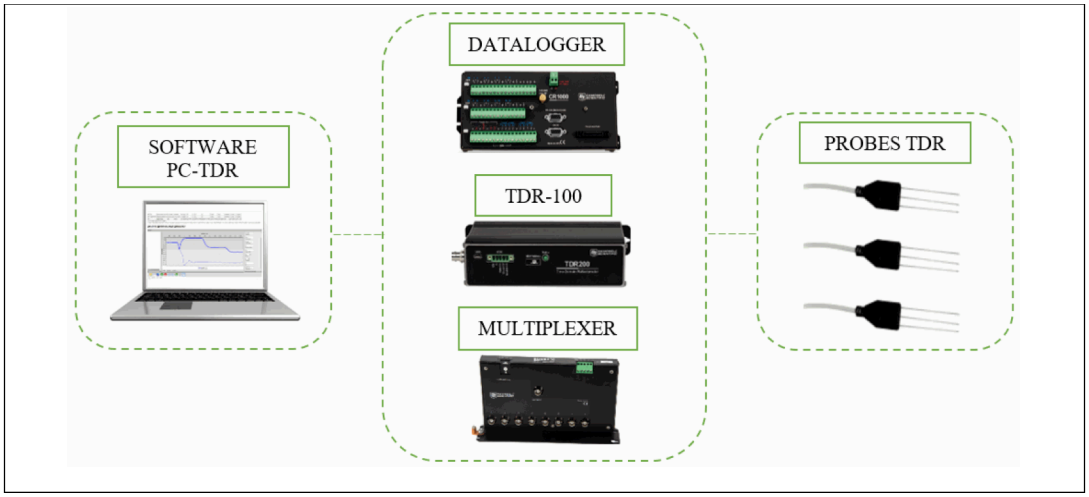

Figure 1. *TDR system*

The velocity of an EM wave (reflection and transmission) over the rods of a TDR probe is shown in the (Equation 3):

$$v = \frac{2\, l_{cal}}{t} \qquad \textbf{(3)}$$

Where:
V = velocity of the EM wave [m/ns];
l_{cal} = rods calibrated length [m];
t = electromagnetic wave travelling time [ns].

In case of low-loss dielectric geological materials and assuming relative magnetic permeability equals to 1 (μ_r = 1, for non-magnetic medium), EM wave propagation velocity (v) is defined by the (Equation 4):

$$v = \frac{c}{\sqrt{\varepsilon_r \cdot \mu_r}} \quad \Rightarrow \quad v = \frac{c}{\sqrt{\varepsilon_r}} \qquad \textbf{(4)}$$

Where:
V = electromagnetic wave velocity [m/ns];
C = velocity of an electromagnetic wave in free space [m/ns];
ε_r = relative dielectric permittivity;
μ_r = relative magnetic permeability ($\mu_r = x_m + 1$);
x_m = magnetic susceptibility.

In an arrangement between (Equation 3) and (Equation 4), dielectric permittivity is shown by (Equation 5):

$$\varepsilon_r = \left(\frac{c \cdot t}{2 l_{cal}} \right)^2 \qquad (5)$$

Where:
ε_r *= relative dielectric permittivity;*
c *= velocity of an EM wave in free space [m/ns];*
t *= EM wave travelling time [ns];*
l_{cal} *= calibrated length of the rods [m].*

3. Methodology

3.1 Sample characterization and classification

Six different types of soils were studied. Soil samples were collected directly from the subgrade during its regularization process. The collection points are located in road works in countryside of the São Paulo State, Brazil (Table 1).

Table 1. *Soil sampling site*

Sample Name	Collection Location	Geographic Coordinates
BRT-1	Campinas City BRT corridor	22°54′36″S 47°05′41″W
BRT-2	Campinas City BRT corridor	22°55′07″S 47°06′28″W
SP-332(S5)	Prof. Zeferino Vaz Highway	22°22′21″S 47°09′52″W
SP-65(S3)	Dom Pedro Highway	22°22′21″S 47°09′52″W
SP-65(S7)	Dom Pedro Highway	22°50′58″S 47°01′42″W
SP-65(S2)	Dom Pedro Highway	22°50′60″S 47°06′24″W

Deformed samples were submitted to tests for characterize its physical properties, as in accordance with the following testing standards: Particle size analysis NBR 7181 (ABNT, 2016d), Determination of specific density NBR 6458 (ABNT, 2016a), Determination of Atterberg Limits NBR 6459 (ABNT, 2016b) and NBR 7180 (ABNT, 2016c). Soil compaction tests were carried out at standard Proctor energy to determine optimum moisture content, maximum dry density and index properties (soil compaction tests as in accordance with NBR 7182 (ABNT, 2016e)). The tests were conducted in the Soil Mechanics Laboratory of the School of Civil Engineering, Architecture and Urban Design, University of Campinas (Unicamp). Finally, the samples were the object of chemical analysis aiming at obtaining the oxides from its constituent elements by means of X-Ray Fluorescence Spectrometry technique at the Laboratory of Analytical Geochemistry of Geosciences Institute, University of Campinas.

(Table 2) shows both physical properties and soil classification as in accordance with "the Highway Research Board" (HRB), "Unified Classification System" (UCS) and Tropical Soils Classification (MCT) (DNER, 1994a); (DNER, 1994b); (DNER, 1996).

Table 2. *Physical properties summary and soil classification*

Sample Name	ρ_{solids} (g/cm^3)	Granulometry (%)			Atterberg Limits (%)			Classification		
		Sand	Silt	Clay	LL	PL	PI	HRB	UCS	MCT
BRT-1	2,75	74	18	8	Non - Plastic			A-2-4	SM	NA'
BRT-2	2,78	67	13	20	25	17	8	A-4	SC	LA'
SP-332 (S5)	2,75	62	13	25	25	14	10	A-6	SC	LG'
SP-65 (S3)	2,85	42	31	27	41	28	14	A-7-6	ML	NG'
SP-65 (S7)	2,80	38	31	31	51	35	16	A-7-5	MH	LG'
SP-65 (S2)	3,01	32	28	40	43	28	15	A-7-6	ML	LG'

ρ_{solids}= Solids specific density, LL = Liquid limit, PL Plastic limit, PI Plasticity index, HRB = Highway Research Board, UCS = Unified Classification System, MCT = Miniature, Compacted Tropical, Tropical soil classification. NA' = Non-lateritic sandy, NG' = Non-lateritic clayey, LA' = Lateritic sandy and LG' = lateritic clayey

(Table 3) shows compaction tests resulting properties. Following, (Table 4) presents a summary of the chemical analyses results with the most relevant oxides, and electric conductivity, for discussion in the present study.

Table 3. *Summary of the properties of compacted soils*

Physical Index	Sample Name					
	BRT-1	BRT-2	SP-332 (S5)	SP-65 (S3)	SP-65 (S7)	SP-65 (S2)
$\rho_{Max.}$ (g/cm^3)	2,06	1,96	1,91	1,72	1,63	1,69
$w_{optimum}$	9,20	11,56	12,54	17,60	22,05	21,97
$\theta_{v\text{-}optimum}$	18,95	22,66	23,95	30,27	35,94	37,14
e	0,33	0,42	0,44	0,66	0,72	0,78

$\rho_{Max.}$= Maximum dry density, $w_{optimum}$= Optimum moisture content, $\theta_{v\text{-}optimum}$= Optimum volumetric moisture content, e = void ratio

Table 4. *Summary of the chemical analysis results*

Oxides (g/100g)	Sample Name					
	BRT-1	BRT-2	SP-332 (S5)	SP-65 (S3)	SP-65 (S7)	SP-65 (S2)
SiO_2	88,38	84,75	79,43	59,83	59,91	42,64
TiO_2	0,28	0,55	1,85	2,01	1,53	4,67
Al_2O_3	6,32	7,80	9,58	18,30	20,43	20,89
Fe_2O_3	1,76	2,81	4,50	10,14	8,07	19,42
E.C. (dS/m)	0,14	0,12	0,10	0,10	0,10	0,10

SiO_2= Silicon dioxide, TiO_2= Titanium dioxide, Al_2O_3= Aluminium oxide, Fe_2O_3= Iron oxide (III), E.C = electric conductivity

3.2 Configuration of TDR Probes and Calibration Columns

Low-cost probes (or guides) were built and calibrated at Non-Destructive Research Laboratory (LIND) of the University of Campinas, to be coupled to the TDR system. The probes consist of three parallel rods 100 mm long and 3 mm in diameter, 15 mm spacing between rods and 1,5 m long coaxial cable. The TDR system used includes a TDR-100 unit, SMDX50 type reading multiplexers and PC-TDR software, all from the Campbell Scientific brand.

Six calibration columns were used, one for each type of soil (Table 2). Each calibration column consists of a PVC cylinder of a 102 mm internal diameter, 190 mm in height and a 5 mm thick wall (Figure 2), placed on a polystyrene base and with 2 TDR probes inserted. The probe geometric configuration and mainly its rods' zone of influence were the main criteria used in column design and sizing. A height of 190 mm was considered in a way, so that the probe head would be protected inside the cylinder. The cylinder wall was drilled with 2 mm diameter holes every 30 mm, to allow for homogeneous moisture loss throughout the sample.

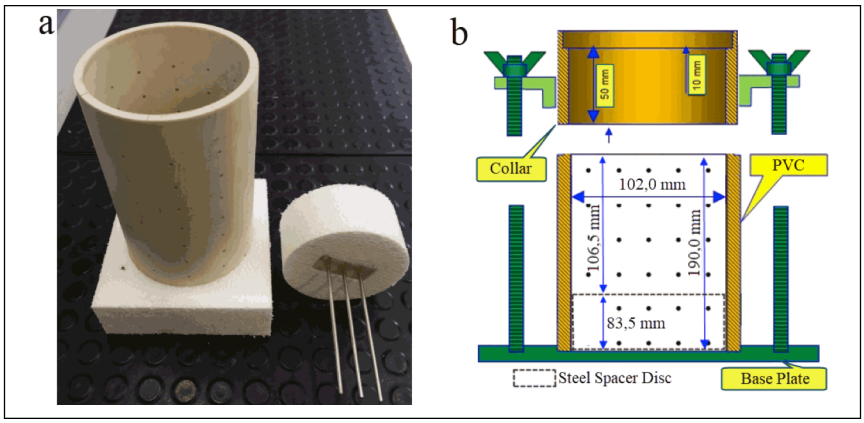

Figure 2. a) PVC cylinder, polystyrene base and TDR probe, and b) Assembly of PVC cylinder between the base plate and collar used in standard Proctor test

3.3. Calibration Columns Preparation and Data Acquisition

The following scheme shows the procedures adopted in the preparation of the calibration columns and data acquisition (Figure 3). Before the compaction process, the mass of the PVC cylinder, probes and polystyrene base were individually determined. A total of 4320 dielectric permittivity observations were recorded (Figure 4).

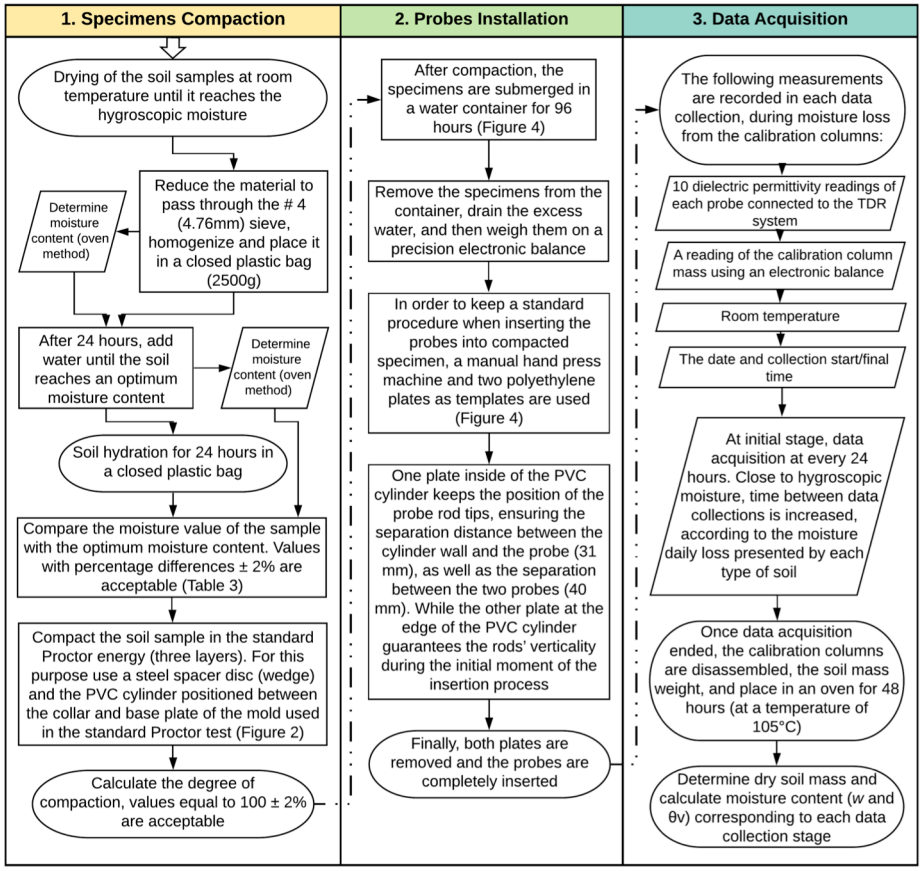

Figure 3. Scheme of procedures implemented in the specimen compaction, TDR probes installation and TDR data acquisition

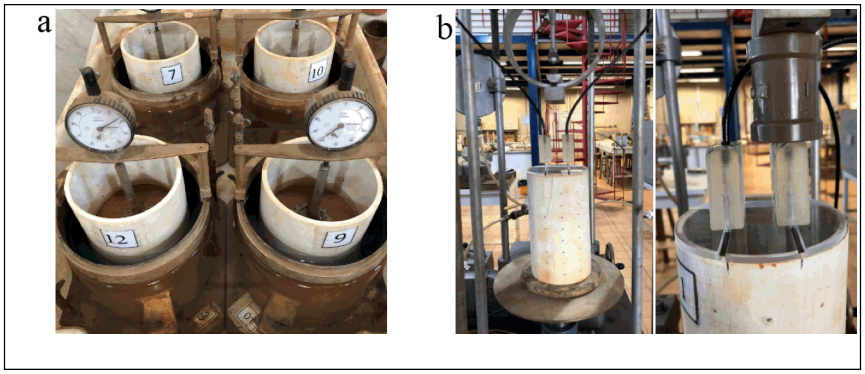

Figure 4. *a) Compacted specimens submerged in water, and b) Probes insertion process, using a manual hand press machine and polyethylene templates*

4. Results and analysis

This section presents the analysis of dielectric permittivity variation as related to moisture content (section 4.1) and it also determines the general calibration model (section 4.2).

4.1 Dielectric permittivity variation in relation to moisture content

(Figure 5) shows the resulting relationship between dielectric permittivity and moisture content for the six soils. A third degree polynomial trend line was used with moisture content (θ_v) as the predictor variable and dielectric permittivity (ε_r) as the response variable.

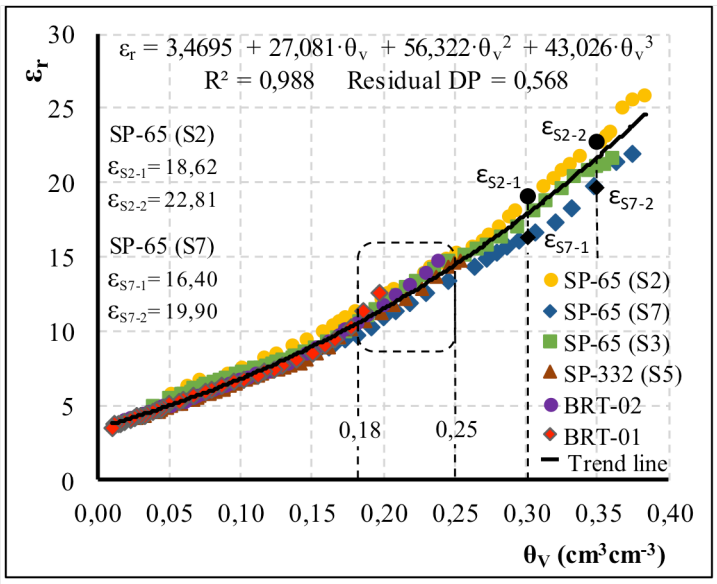

Figure 5. Relationship between dielectric permittivity and moisture content, considering all soils studied

The third degree polynomial trend line presented the highest determination coefficient (R^2 = 0,988) and the lowest standard deviation of the residuals (SD = 0,568). From this relationship, small permittivity variations for the same moisture value are highlighted (specially to the left of θ_v = 0,25 cm^3cm^{-3} in (Figure 5), even though they are soils with different textures and different physical properties (Table 2) and (Table 3). To the right of θ_v = 0,25 cm^3cm^{-3}, the soils presented more distinctive permittivity differences for the same moisture content.

It is known that dielectric permittivity measurement is directly influenced by the various ways which different types of soils interact in the presence of water. The causes of permittivity differences highlighted before are mainly due to the influence of the soils mineralogical composition and, to a lesser extent, to the influence of their texture.

4.1.1 Soil texture influence

It can be noted in (Figure 5) that, between the moisture contents of 0,18 to 0,25 cm^3cm^{-3} (square with dashed lines) the soils with the highest sand fraction (BRT-1, BRT-2 and SP-332 (S5)), showed dielectric permittivity values slightly higher than soils with a higher fraction of silt and clay (SP-65 (S2), SP-65 (S7) and SP-65 (S3)). As can be seen in (Table 3), the soils BRT-1, BRT-2 and SP-332 (S5) reached their optimum moisture content in this moisture range. This led to a greater contribution of the water phase (ε_{water}= 81) and, consequently, to an increase in the measurement of dielectric permittivity. Outside this range (0,18 to 0,25 cm^3cm^{-3}), the influence of the mineralogical composition was dominant.

4.1.2 Influence of the soils' mineralogical composition

According to the chemical analysis results (Table 4), the six soils show a greater proportion of four oxides, common in tropical soils: SiO_2, TiO_2, Al_2O_3 and Fe_2O_3. Being Fe_2O_3 the oxide that most influence dielectric permittivity determination with TDR, given their magnetic properties. This influence was observed in (Figure 5) in the dielectric permittivity measured for moisture contents less than 0,18 cm^3cm^{-3}, where the SP-65 (S2), SP-65 (S3) and SP-65 (S7) soils with a higher proportion of Fe_2O_3, showed moderately higher dielectric permittivity values than the BRT-1, BRT-2 and SP-332 (S5) soils with a lower proportion of this oxide. The Fe_2O_3 influence was clearly more evident for moisture contents greater than 0,25 cm^3cm^{-3}. It is highlighted from (Figure 5), the increase in the differences between the dielectric permittivity values as the moisture increases. For example, in moistures close to optimum moisture content of soils SP-65(S2) and SP-65(S7), percentage differences between dielectric permittivity values was 13,5% for θ_v = 0,30 cm^3cm^{-3} (points ε_{S2-1} and ε_{S7-1}) and 14,6% for θ_v = 0,35 cm^3cm^{-3} (points ε_{S2-2} and ε_{S7-2}).

Data obtained from TDR indicated an increase in the reflection travelling time (t) of the electromagnetic wave, especially in case of soils with a higher proportion of Fe_2O_3. Therefore, in this study, the increment in the reflection travelling time indicates that magnetic permeability shows values above the unit ($\mu_r > 1$), according with (Equation 6). This was expected due to the presence of minerals with magnetic susceptibility different from zero ($x_m > 0$). Additionally, energy loss due to conductivity was disregarded, given the low electric conductivity of soils (Table 4). Hence, relative dielectric permittivity corresponds to a fraction of the estimated value when using TDR, which matches the mathematical approach purposed by (Roth et al., 1990).

$$\varepsilon_r \cdot \mu_r = \left(\frac{c \cdot t}{2\, l_{cal}} \right)^2 \quad \Rightarrow \quad \varepsilon_r = \frac{\left(\frac{c \cdot t}{2\, l_{cal}} \right)^2}{\mu_r} \qquad \textbf{(6)}$$

Where:
ε_r= relative dielectric permittivity;
μ_r= relative magnetic permeability;
c= velocity of an EM wave in free space [m/ns];
t= EM wave travelling time [ns];
l_{cal}= rods calibrated length [m].

Similar results were obtained by (Robinson et al., 1994), which studied the influence of some magnetic minerals in determining dielectric permittivity using TDR as well as in subsequent moisture content estimates.

4.2 General calibration model

(Table 5) shows the general calibration model developed considering the six soils and two specific models grouping the soils into fine and coarse (classification (Table 2)). Each model was determined by using a third degree polynomial regression, with dielectric permittivity (ε_r) as predictor variable and moisture content (θ_v) as response variable.

Table 5. *Calibration models developed with their respective statistical indicators*

Model	**Coefficients $\theta_v = a + b\varepsilon_r + c\varepsilon_r^2 + d\varepsilon_r^3$**				**R^2**	**SD Residues (cm^3cm^{-3})**
	a	**b**	**c**	**d**		
General	$-1{,}10 \times 10^{-1}$	$3{,}71 \times 10^{-2}$	$-1{,}02 \times 10^{-3}$	$1{,}28 \times 10^{-5}$	0,990	0,0096
Fine	$-1{,}27 \times 10^{-1}$	$3{,}86 \times 10^{-2}$	$-1{,}01 \times 10^{-3}$	$1{,}11 \times 10^{-5}$	0,986	0,0116
Coarse	$-1{,}53 \times 10^{-1}$	$5{,}22 \times 10^{-2}$	$-2{,}40 \times 10^{-3}$	$4{,}73 \times 10^{-5}$	0,996	0,0039

It is distinguished from (Table 5), that the achieved accuracy in this study can be compared (standard deviation (SD)), with the accuracy mentioned by: (Topp et al., 1980) of 0,013 cm^3cm^{-3}, (Ledieu et al.,1986) of 0,0076 cm^3cm^{-3}, (Roth et al., 1992) of 0,015 cm^3cm^{-3} and (Jacobsen and SchjØnning, 1993) of 0,0097 cm^3cm^{-3}. It should be noted that calibration models which involve coarse soils, commonly present better adjustments (higher R^2 and lower SD). This same trend was observed in the works developed by (Topp et al., 1980), (Sarani and Afrasjab, 2012), (Dos Santos Batista et al., 2016) and (Costa, 2017).

(Figure 6) presents the adjusted curve using the general calibration model, for comparison with adjusted curves through the classic equations of (Topp et al., 1980) (Equation 1) and (Ledieu et al., 1986) (Equation 2), both models being accepted by the scientific community and widely used in practical terms.

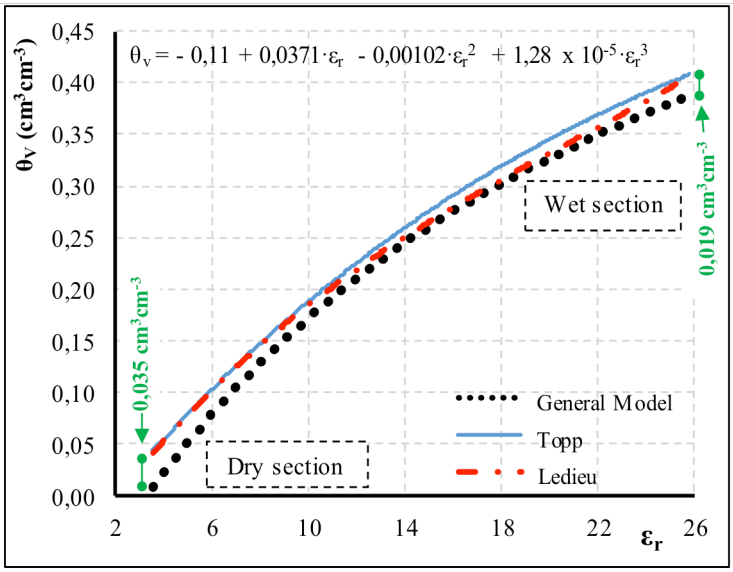

Figure 6. Comparison of the adjusted curve through the general calibration model with the adjusted curves using (Topp et al., 1980) and (Ledieu et al., 1986) models

As can be seen in (Figure 6), both the model of (Topp et al., 1980) as the model of (Ledieu et al., 1986), overestimate the moisture content for the same dielectric permittivity value. Mainly at the beginning in the dry section and at the end in the wet section of the curves, with differences of 0,035 cm^3cm^{-3} (percentage difference of 385,4%) and of 0,019 cm^3cm^{-3} (percentage difference of 5,1%), respectively.

The differences in the moisture content prediction are mostly due to: **a)** mineralogical composition influence of the soils used to develop the general model, especially fine soils that show magnetic susceptibility (approached in section 4.1.2). About this, (Roth et al., 1992) and (Robinson et al. (1994) emphasized that calibrated models with soils that have shown susceptibility in the presence of an electromagnetic field can differ from those that were validated for not magnetic mineral soils, thus leading to an overestimation of moisture content. **b)** Dry density used in the general calibration model was between 1,63 - 2,06 g cm^{-3} (Table 3), in contrast to Topp (1,04 - 1,44 g cm^{-3}) and Ledieu (1,38 - 1,78 g cm^{-3}) that used lower dry density values. The high density of the soils led to a lower void ratio (*e*), which enabled a greater contribution of solid phase ($\varepsilon_{particle}$= 3-5) in the final determination of the soil dielectric permittivity. Consequently, it was observed a decrease in the contribution of air phase (ε_{air}= 1) in the dry section (low moisture) and a reduction of the liquid phase influence (ε_{water}= 81) in the wet section (high moisture). Being the high density effect more evident on the dry section of the adjusted curve (Figure 6). It is a general consensus among researchers that dielectric permittivity can be influenced by the dry density of the soil. The increase in density results in an increase in the dielectric permittivity for low moisture contents (Jacobsen and SchØnning, 1993); (Gong et al., 2003); (Namdar-Khojasteh et al., 2012).

5. Conclusions

According to the results analysed in this study, the implemented laboratory procedures were shown to be effective in establishing through calibration models, the relationship between dielectric permittivity and moisture variation in compacted tropical soils. The calibration models developed enable the application of non-destructive techniques (TDR and GPR) in estimating and monitoring moisture content accurately and in accordance with the geotechnical characteristics of the subgrade. It should be underscored that correctly calibrated models for engineering specific applications not only need standardized processes and well calibrated equipment but also require a careful selection and grouping of the soils; considering their physical properties according to their use, in addition to their mineralogical composition.

It was found the influence of magnetic susceptibility of tropical soils in determining dielectric permittivity and, as a consequence in moisture estimates, thus reaffirming the need of specific calibrations for these types of soils.

Furthermore, it was also concluded that validated models for not magnetic mineral soils and with lower density, overestimate moisture content. The combined effect of magnetic susceptibility and the high density of the soils was evident in reading and acquisition of data using TDR. The effect of magnetic susceptibility was observed throughout the relationships between dielectric permittivity and moisture content in the general model, nevertheless, with a dominant effect on the wet section (high moisture). In the case of the high density its effect was dominant on the dry section (low moisture) of the model

6. References

ABNT (2016a). NBR 6458 – Grãos de pedregulho retidos na peneira de abertura 4,8mm – determinação da massa específica, da massa específica aparente e da absorção de água. Associação Brasileira de Normas Técnicas, Rio de Janeiro.

ABNT (2016b). NBR 6459 – Solo – determinação do limite de liquidez. Associação Brasileira de Normas Técnicas, Rio de Janeiro.

ABNT (2016c). NBR 7180 – Solo – determinação do limite de plasticidade. Associação Brasileira de Normas Técnicas, Rio de Janeiro.

ABNT (2016d). NBR 7181 – Solo – análise granulométrica. Associação Brasileira de Normas Técnicas, Rio de Janeiro.

ABNT (2016e). NBR 7182 – Solo – ensaio de compactação. Associação Brasileira de Normas Técnicas, Rio de Janeiro.

Al-Qadi, I.; Lahouar, S.; Loulizi, A.; Elseifi, M.; Wilkes, J. (2004). Effective approach to improve pavement drainage layers. Journal of Transportation Engineering, 130(5): 658–664, doi: 10.1061/(ASCE)0733-947X(2004)130:5(658).

Bastos, J. (2013). Influência da variação da umidade no comportamento de pavimentos da região metropolitana de Fortaleza. Fortaleza: Universidade Federal do Ceará.

Benedetto, A. (2010). Water content evaluation in unsaturated soil using GPR signal analysis in the frequency domain. Journal of Applied Geophysics, 71(1): 26–35, doi: https://doi.org/10.1016/j.jappgeo.2010.03.001.

Benedetto, A.; Tosti, F.; Ortuani, B.; Giudici, M.; Mele, M. (2015). Mapping the spatial variation of soil moisture at the large scale using GPR for pavement applications. Near Surface Geophysics, 13(3): 269–278, doi: https://doi.org/10.3997/1873-0604.2015006.

Bhuyan, H.; Scheuermann, A.; Bodin, D.; Becker, R. (2018). Soil moisture and density monitoring methodology using TDR measurements. International Journal of Pavement Engineering, 1–12, doi: https://doi.org/10.1080/10298436.2018.1537491.

Bittelli, M.; Salvatorelli, F.; Pisa, P. (2008). Correction of TDR-based soil water content measurements in conductive soils. Geoderma, 143(1): 133–142, doi: https://doi.org/10.1016/j.geoderma.2007.10.022.

Costa, B. (2017). Reflectometria no domínio do tempo (TDR) para determinação do conteúdo de água em solos tropicais do Distrito Federal. Brasília/DF: Universidade de Brasília.

Curioni, G.; Chapman, D.; Metje, N. (2017). Seasonal variations measured by TDR and GPR on an anthropogenic sandy soil and the implications for utility detection. Journal of Applied Geophysics, 141(Supplement C): 34–46, doi: https://doi.org/10.1016/j.jappgeo.2017.01.029.

DNER (1994a). DNER-ME 256/94: Solos compactados com equipamento miniatura - determinação da perda de massa por imersão. Departamento Nacional de Estradas de Rodagem, Rio de Janeiro.

DNER (1994b). DNER-ME 258/94: Solos compactados com equipamento miniatura – Mini-MCV. Departamento Nacional de Estradas de Rodagem, Rio de Janeiro.

DNER (1996). DNER-CLA 259/96: Solos compactados com equipamento miniatura – Mini-MCV. Departamento de Nacional Estradas de Rodagem, Rio de Janeiro.

Dos Santos Batista, L.; Coelho, F.; Pereira, F.; Da Silva, M.; Gomes Filho, R.; Gonçalves, A. (2016). Calibração de sonda artesanal de uso com TDR para avaliação de umidade de solos. Revista Brasileira de Agricultura Irrigada, 10(2): 522-532, doi: 10.7127/rbai.v10n200388.

Ekblad, J.; Isacsson, U. (2007). Time-domain reflectometry measurements and soil-water characteristic curves of coarse granular materials used in road pavements. Canadian Geotechnical Journal, 44(7): 858–872, doi: https://doi.org/10.1139/t07-024.

Fernandes, F.; Fernandes, A.; Pais, J. (2017). Assessment of the density and moisture content of asphalt mixtures of road pavements. Construction and Building Materials, 154: 1216–1225, doi: https://doi.org/10.1016/j.conbuildmat.2017.06.119.

Friedman, S. (2011). Electrical Properties of Soils. In: Glinski, J.; Horabik, J. and Lipiec, J. (Eds.) Encyclopedia of Agrophysics. Dordrecht: Springer Netherlands, pp. 242–255.

Gong, Y.; Cao, Q.; Sun, Z. (2003). The effects of soil bulk density, clay content and temperature on soil water content measurement using time-domain reflectometry. Hydrological Processes, 17(18): 3601–3614, doi: https://doi.org/10.1002/hyp.1358.

Huisman, J.; Hubbard, S.; Redman, J.; Annan, A. (2003). Measuring Soil Water Content with Ground Penetrating Radar. Vadose Zone Journal, 2(4): 476–491, doi: https://doi.org/10.2113/2.4.476.

Jacobsen, O.; SchjØnning, P. (1993). A laboratory calibration of time domain reflectometry for soil water measurement including effects of bulk density and texture. Journal of Hydrology, 151(2–4): 147–157, https://doi.org/10.1016/0022-1694(93)90233-Y.

Jiang, Y.; Tayabji, S. (1999). Evaluation of in situ moisture content at long-term pavement performance seasonal monitoring program sites. Transportation Research Record: Journal of the Transportation Research Board, 1655(99–0395): 118–126, doi: https://doi.org/10.3141/1655-16.

Jones, S.; Wraith, J.; Or, D. (2002). Time domain reflectometry measurement principles and applications. Hydrological processes, 16(1): 141–153, doi: https://doi.org/10.1002/hyp.513. 286 Revista Ingeniería de Construcción Vol 35 Nº3 Diciembre de 2020 www.ricuc.cl

Khakiev, Z.; Shapovalov, V.; Kruglikov, A.; Morozov, A.; Yavna, V. (2014). Investigation of long term moisture changes in trackbeds using GPR. Journal of Applied Geophysics, 110(Supplement C): 1–4, doi: https://doi.org/10.1016/j.jappgeo.2014.08.014.

Klemunes, J. (1998). Determining soil volumetric moisture content using time domain reflectometry. FHWA-RD-97-I 39. United States. Federal Highway Administration. Office of Engineering Research and Development. p. 74.

Ledieu, J.; De Ridder, P.; De Clerck, P.; Dautrebande, S. (1986). A method of measuring soil moisture by time-domain reflectometry. Journal of Hydrology, 88(3–4): 319–328, doi: https://doi.org/10.1016/0022-1694(86)90097-1.

Logsdon, S. (2006). Experimental limitations of time domain reflectometry hardware for dispersive soils. Soil Science Society of America Journal, 70(2): 537–540, doi: https://doi.org/10.2136/sssaj2005.0176N.

Namdar-Khojasteh, D.; Shorafa, M.; Omid, M. (2012). Evaluation of dielectric constant by clay mineral and soil physico-chemical properties. African journal of Agricultural research, 7(2): 170–176, doi: 10.5897/AJAR10.346.

Robinson, D.; Bell, J.; Batchelor, C. (1994). Influence of iron and titanium on water content determination by TDR. In: Time domain reflectometry applications in soil science held at the research centre foulum, Denmark, pp. 63–70.

Roth, C.; Malicki, M.; Plagge, R. (1992). Empirical evaluation of the relationship between soil dielectric constant and volumetric water content as the basis for calibrating soil moisture measurements by TDR. European Journal of Soil Science, 43(1): 1–13, doi: https://doi.org/10.1111/j.1365-2389.1992.tb00115.x.

Roth, K.; Schulin, R.; Flühler, H.; Attinger, W. (1990). Calibration of time domain reflectometry for water content measurement using a composite dielectric approach. Water Resources Research, 26(10): 2267–2273, doi: https://doi.org/10.1029/WR026i010p02267.

Saarenketo, T. (1998). Electrical properties of water in clay and silty soils. Journal of Applied Geophysics, 40(1): 73–88, doi: https://doi.org/10.1016/S0926-9851(98)00017-2.

Saarenketo, T. (2006). Electrical properties of road materials and subgrade soils and the use of Ground Penetrating Radar in traffic infrastructure surveys. Oulu: University of Oulu.

Sarani, N.; Afrasjab, P. (2012). Effect of soil texture on moisture measurement accuracy with Theta probe ML2 in Sistan region. In: International conference on chemical, ecology and environmental sciences. Bangkok, pp. 114 - 177.

Souza, C.; Matsura, E.; Testezlaf, R. (2001). Application of the TDR technique in tropical soil. TDR 2001 Proceedings. Northwestern University. Evanston, IL, p. 273–280.

Stangl, R.; Buchan, G.; Loiskandl, W. (2009). Field use and calibration of a TDR-based probe for monitoring water content in a high-clay landslide soil in Austria. Geoderma, 150(1–2): 23–31, doi: https://doi.org/10.1016/j.geoderma.2009.01.002.

Thring, L.; Boddice, D.; Metje, N.; Curioni, G.; Chapman, D.; Pring, L. (2014). Factors affecting soil permittivity and proposals to obtain gravimetric water content from time domain reflectometry measurements. Canadian Geotechnical Journal, 51(11): 1303–1317, doi: https://doi.org/10.1139/cgj-2013-0313.

Topp, G.; Davis, J.; Annan, A. (1980). Electromagnetic determination of soil water content: Measurements in coaxial transmission lines. Water resources research, 16(3): 574–582, doi: https://doi.org/10.1029/WR016i003p00574.

Tosti, F.; Slob, E. (2015). Determination, by using GPR, of the volumetric water content in structures, substructures, foundations and soil. In: Benedetto, A. and Pajewski, L. (Eds.). Civil Engineering Applications of Ground Penetrating Radar. Switzerland: Springer. pp. 163–194.

.